

nature

The Living Record of Science

《自然》百年科学经典

(英汉对照版)

第十卷

总顾问：李政道 (Tsung-Dao Lee)

英方主编：Sir John Maddox 中方主编：路甬祥
Sir Philip Campbell

X 2002-2007

VIII 1993-1997

IX 1998-2001

VII 1983-1992

VI 1973-1982

V 1963-1972

IV 1946-1962

III 1934-1945

II 1931-1933

I 1902-1930

外语教学与研究出版社 · 麦克米伦教育 · 自然科研

FOREIGN LANGUAGE TEACHING AND RESEARCH PRESS · MACMILLAN EDUCATION · NATURE RESEARCH

nature

The Living Record of Science

《自然》百年科学经典



(英汉对照版)

第十卷

总顾问：李政道 (Tsung-Dao Lee)

英方主编：Sir John Maddox 中方主编：路甬祥
Sir Philip Campbell



外语教学与研究出版社 · 麦克米伦教育 · 自然科研

FOREIGN LANGUAGE TEACHING AND RESEARCH PRESS · MACMILLAN EDUCATION · NATURE RESEARCH

北京 BEIJING

Original English Text © Macmillan Publishers Limited
Chinese Translation © Foreign Language Teaching and Research Press

This edition is published under arrangement with Macmillan Publishers (China) Limited. It is for sale in the People's Republic of China only, excluding Hong Kong SAR, Macao SAR and Taiwan Province, and may not be bought for export therefrom.

图书在版编目 (CIP) 数据

《自然》百年科学经典. 第十卷, 2002—2007: 英汉对照 / (英) 约翰·马多克斯 (John Maddox), (英) 菲利普·坎贝尔 (Philip Campbell), 路甬祥主编. — 北京: 外语教学与研究出版社, 2019.8

ISBN 978-7-5213-1167-9

I. ①自… II. ①约… ②菲… ③路… III. ①自然科学—文集—英、汉 IV. ①N53

中国版本图书馆 CIP 数据核字 (2019) 第 189358 号

地图审图号: GS (2019) 3264 号

出版人 徐建忠
项目统筹 章思英
项目负责 刘晓楠 黄小斌
责任编辑 王丽霞
责任校对 黄小斌
封面设计 孙莉明 曹志远
版式设计 孙莉明
出版发行 外语教学与研究出版社
社 址 北京市西三环北路 19 号 (100089)
网 址 <http://www.fltrp.com>
印 刷 北京华联印刷有限公司
开 本 787 × 1092 1/16
印 张 67
版 次 2019 年 9 月第 1 版 2019 年 9 月第 1 次印刷
书 号 ISBN 978-7-5213-1167-9
定 价 568.00 元

购书咨询: (010) 88819926 电子邮箱: club@fltrp.com

外研书店: <https://waiyants.tmall.com>

凡印刷、装订质量问题, 请联系我社印制部

联系电话: (010) 61207896 电子邮箱: zhijian@fltrp.com

凡侵权、盗版书籍线索, 请联系我社法律事务部

举报电话: (010) 88817519 电子邮箱: banquan@fltrp.com

物料号: 311670001



记载人类文明
沟通世界文化
www.fltrp.com

《自然》百年科学经典（英汉对照版）

总顾问：李政道（Tsung-Dao Lee）

英方主编：Sir John Maddox 中方主编：路甬祥

Sir Philip Campbell

编审委员会

英方编委

Philip Ball

Vikram Savkar

David Swinbanks

中方编委（以姓氏笔画为序）

许智宏

赵忠贤

滕吉文

本卷审稿专家（以姓氏笔画为序）

于 军	王 宇	王晓良	尹凤玲	冯珑珑	邢 松	刘冬生
许 冰	李 然	肖景发	张颖奇	陆培祥	陈含章	陈继征
季江徽	周济林	郑旭峰	胡永云	胡松年	夏俊卿	徐 栋
徐文堪	高树基	曹 俊	曹庆宏	常 江	曾长青	蔡荣根
裴端卿	黎 卓	潘 雷				

编译委员会

本卷翻译工作组稿人 (以姓氏笔画为序)

王丽霞	王晓蕾	王耀杨	刘明	刘晓楠	关秀清	李琦
何铭	周家斌	郭红锋	黄小斌	蔡则怡		

本卷翻译人员 (以姓氏笔画为序)

王耀杨	毛晨晖	田晓阳	吕静	吕孟珍	任奕	刘项琨
刘皓芳	齐红艳	安宇森	孙惠南	李平	李梅	李辉
肖莉	何钧	汪浩	张瑶楠	金世超	周杰	周家斌
郭思彤	梁恩思	韩然	谭秀慧			

本卷校对人员 (以姓氏笔画为序)

刘雨佳	张玉光	陈思原	周少贞	贺舒雅	夏洁媛	顾海成
郭思彤	黄小斌	蔡则怡	潘卫东	Eric Leher (澳)		

Contents

目录

Estimating the Human Health Risk from Possible BSE Infection of the British Sheep Flock	2
英国羊群可能的BSE感染带来的人类健康风险评估	3
The Role of the Thermohaline Circulation in Abrupt Climate Change	24
温盐环流在气候突变中的作用	25
Detecting Recent Positive Selection in the Human Genome from Haplotype Structure	52
从单倍型结构检测人类基因组近期的正选择	53
Initial Sequencing and Comparative Analysis of the Mouse Genome	74
小鼠基因组的初步测序和对比分析	75
Detection of Polarization in the Cosmic Microwave Background Using DASI	160
利用DASI探测宇宙微波背景的偏振	161
Upper Limits to Submillimetre-range Forces from Extra Space-time Dimensions	236
来自额外空间维度在亚毫米尺度上力程的上限	237
An Extended Upper Atmosphere Around the Extrasolar Planet HD209458b	252
太阳系外行星HD209458b扩展的高层大气研究	253
The Principle of Gating Charge Movement in a Voltage-dependent K^+ Channel	268
电压依赖性 K^+ 通道的门控电荷运动的原理	269
The International HapMap Project	294
国际人类基因组单体型图计划	295
A Correlation between the Cosmic Microwave Background and Large-scale Structure in the Universe	320
宇宙微波背景和大尺度结构的相关	321
Mice Cloned from Olfactory Sensory Neurons	332
从嗅觉神经元克隆小鼠	333
A Precision Measurement of the Mass of the Top Quark	358
顶夸克质量的精确测量	359

Genetic Evidence Supports Demic Diffusion of Han Culture	374
遗传学证据支持汉文化的扩散源于人口扩张	375
A New Small-bodied Hominin from the Late Pleistocene of Flores, Indonesia	390
印度尼西亚弗洛勒斯晚更新世一身材矮小人族新成员	391
Unusual Activity of the Sun during Recent Decades Compared to the Previous 11,000 Years	420
最近几十年太阳活动的异动：与过去的11,000年相比	421
Tomographic Imaging of Molecular Orbitals	436
分子轨道的层析成像	437
Stratigraphic Placement and Age of Modern Humans from Kibish, Ethiopia	462
来自埃塞俄比亚基比什的现代人的地层位置和年代	463
The DNA Sequence of the Human X Chromosome	480
人类X染色体的DNA序列	481
Infrared Radiation from an Extrasolar Planet	532
来自一颗系外行星的红外辐射	533
Origin of the Cataclysmic Late Heavy Bombardment Period of the Terrestrial Planets	546
类地行星激变晚期重轰击期的起源	547
Experimental Investigation of Geologically Produced Antineutrinos with KamLAND	562
KamLAND对地质来源的反中微子的实验研究	563
First Fossil Chimpanzee	582
第一个黑猩猩化石	583
Molecular Insights into Human Brain Evolution	598
从分子角度洞察人类大脑的演化	599
Anthropogenic Ocean Acidification over the Twenty-first Century and Its Impact on Calcifying Organisms	612
21世纪人类活动引起的海洋酸化效应及其对钙质生物的影响	613
Characterization of the 1918 Influenza Virus Polymerase Genes	638
1918年流感病毒聚合酶基因的特点	639

Implications for Prediction and Hazard Assessment from the 2004 Parkfield Earthquake	658
从2004年帕克菲尔德地震看地震预测和灾害评估的启示	659
A Haplotype Map of the Human Genome	684
人类基因组的单体型图谱	685
Rain, Winds and Haze during the Huygens Probe's Descent to Titan's Surface	772
惠更斯空间探测器下落至土卫六表面过程中的雨、风和雾霾	773
Discovery of a Cool Planet of 5.5 Earth Masses through Gravitational Microlensing	836
通过微引力透镜发现一颗5.5倍地球质量的冷行星	837
Folding DNA to Create Nanoscale Shapes and Patterns	848
折叠DNA以形成纳米尺度的形状和图案	849
Long γ -ray Bursts and Core-collapse Supernovae Have Different Environments	872
长伽马射线暴与核坍缩超新星具有不同的环境	873
The Association of GRB 060218 with a Supernova and the Evolution of the Shock Wave	894
GRB 060218与一个超新星成协以及激波的演化	895
Analysis of One Million Base Pairs of Neanderthal DNA	906
对尼安德特人DNA的一百万碱基对的分析	907
Identification and Analysis of Functional Elements in 1% of the Human Genome by the ENCODE Pilot Project	936
通过ENCODE先导计划鉴定与分析人类基因组1%区域内的功能元件	937
Generation of Germline-competent Induced Pluripotent Stem Cells	1008
具有种系功能的诱导多能干细胞的产生	1009
<i>In Vitro</i> Reprogramming of Fibroblasts into a Pluripotent ES-cell-like State	1032
体外重编程技术将成纤维细胞诱导到ES样细胞的多能性状态	1033
Appendix: Index by Subject	
附录: 学科分类目录	1061

Volume X
(2002-2007)

Estimating the Human Health Risk from Possible BSE Infection of the British Sheep Flock

N. M. Ferguson *et al.*

Editor's Note

The neurodegenerative disease bovine spongiform encephalopathy (BSE) was first recognized in British cattle in the 1980s. The government's response was to monitor herds closely and restrict beef sales to ensure that organs known to harbour BSE were not sold. Nevertheless, an outbreak occurred in the late 1980s, leading to the culling of British cattle and a European ban on British beef exports. BSE is believed to trigger a similar, fatal disease in humans called Creutzfeldt-Jakob disease, of which more than 160 people have died following the 1980s BSE outbreak. Here epidemiologist Roy Anderson and colleagues model the likely course of the human epidemic and predict future deaths to be in the range 50–50,000.

Following the controversial failure of a recent study¹ and the small numbers of animals yet screened for infection², it remains uncertain whether bovine spongiform encephalopathy (BSE) was transmitted to sheep in the past via feed supplements and whether it is still present. Well grounded mathematical and statistical models are therefore essential to integrate the limited and disparate data, to explore uncertainty, and to define data-collection priorities. We analysed the implications of different scenarios of BSE spread in sheep for relative human exposure levels and variant Creutzfeldt-Jakob disease (vCJD) incidence. Here we show that, if BSE entered the sheep population and a degree of transmission occurred, then ongoing public health risks from ovine BSE are likely to be greater than those from cattle, but that any such risk could be reduced by up to 90% through additional restrictions on sheep products entering the food supply. Extending the analysis to consider absolute risk, we estimate the 95% confidence interval for future vCJD mortality to be 50 to 50,000 human deaths considering exposure to bovine BSE alone, with the upper bound increasing to 150,000 once we include exposure from the worst-case ovine BSE scenario examined.

THE aim of this study was not to evaluate the probability that BSE has entered the sheep flock, but rather, given the pessimistic assumption that infection has occurred, to explore its potential extent and pattern of spread. In this, we used epidemiological parameter estimates from experimental BSE infections of sheep, and, where data are unavailable, assumed (given the observed similarities in BSE and scrapie pathogenesis in sheep) that other aspects of disease epidemiology resemble those of scrapie. Analyses were constrained to be consistent with the failure to detect the BSE agent in a small sample of 180 brains² collected between 1996 and 2000 from sheep diagnosed with scrapie (giving

英国羊群可能的 BSE 感染带来的人类健康风险评估

弗格森等

编者按

神经退行性疾病牛海绵状脑病 (BSE) 于 20 世纪 80 年代首次在英国牛中发现。英国政府的回应是密切监控牧群，限制牛肉销售，以确保患有 BSE 的牛的器官不被出售。然而，20 世纪 80 年代末爆发了一场疫情，导致英国牲畜遭到扑杀，欧洲禁止英国牛肉出口。据信，BSE 在人类中引发了一种类似的致命疾病 (称为克雅氏病)。自 20 世纪 80 年代 BSE 爆发以来，已有 160 多人死于这种疾病。流行病学家罗伊·安德森和他的同事们模拟了人类流行病的可能进程，并预测未来因这种疾病死亡的人数将在 50 ~ 50,000 之间。

随着最近一项有争议的研究的失败^[1] 加上少数动物已经接受过感染筛查^[2]，但牛海绵状脑病 (BSE) 过去是否是通过饲料添加剂传染到羊身上以及现在是否仍然存在都还不能确定。因此，有充分依据的数学和统计学模型对于整合有限的不同数据、探索不确定性以及确定数据收集的重点都是十分必要的。我们分析了 BSE 在羊群中传播的不同方式与相关的人类暴露水平以及变异型克雅氏病 (vCJD) 患病率之间的关系，我们发现，如果 BSE 进入了羊群并且发生了一定程度的传播，那么羊 BSE 导致的不断增加的公共卫生风险很可能比牛的大，但是通过附加限制羊产品进入食物供应，可以将任何这类风险减少高达 90%。将这个分析延伸到绝对风险，在 95% 置信区间内，我们估计单纯暴露于牛 BSE 的未来 vCJD 死亡率是 50 到 50,000 人，而一旦暴露于最坏方式传播的羊 BSE，则上限增加到 150,000 人。

本研究的目的是不是评估 BSE 进入羊群的可能性，而是悲观地假设感染已经发生，以此来研究感染传播的潜在程度和方式。在本文中，我们使用了实验羊的 BSE 感染得出的流行病学参数估计，对于那些无法获得的数据，就假定该病流行病学的这些数据与瘙痒病类似 (考虑到羊身上 BSE 和瘙痒病发病机理的相似性)。此次分析的是从 1996 年到 2000 年之间患有瘙痒病的羊中收集的 180 份脑标本^[2]，要求在这些脑标本中不能检测到 BSE 病原体的存在 (考虑到在明显患有瘙痒病的绵羊

an upper bound for BSE prevalence within apparently scrapie-affected sheep of 2%; Fig. 1a), and are also broadly consistent with an assessment of historical exposure of the ovine population to meat and bonemeal (MBM)³.

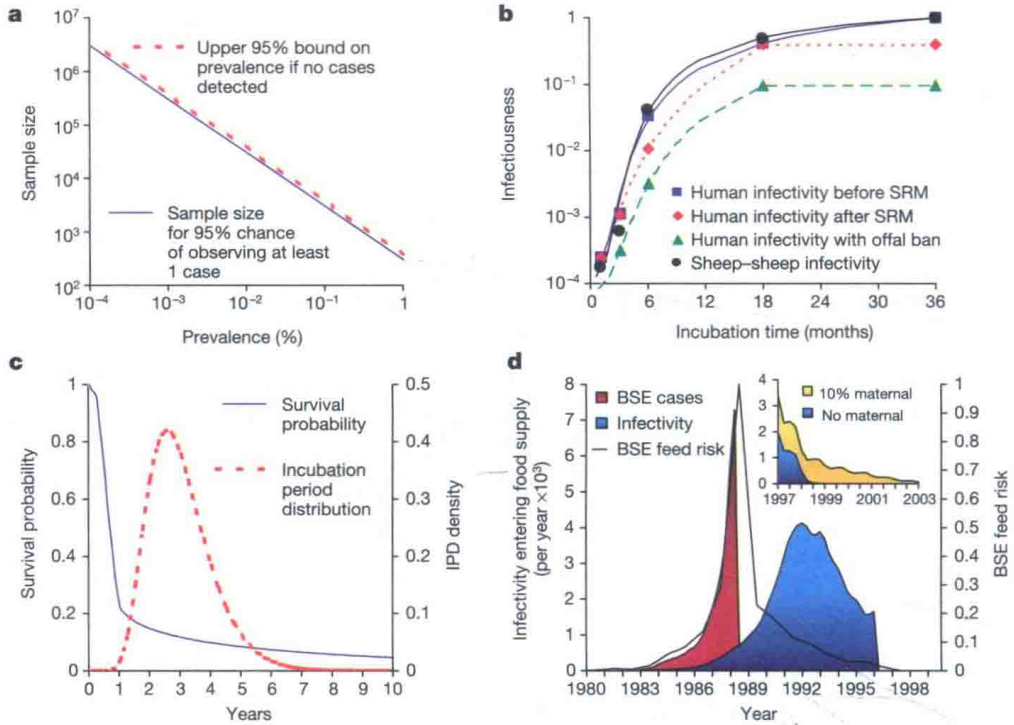


Fig. 1. Epidemiological inputs to transmission model. **a**, Relationship between sample size and detectable prevalence in screening studies. **b**, Infectiousness of sheep as a function of time from infection (see Methods). Sheep and human profiles are separately normalized to give maxima of 1. **c**, Survival probability of sheep as a function of age, and assumed incubation period distribution (IPD) of BSE in sheep. The survivorship function was estimated from annual data from the June census, slaughter, export and disappearance statistics, and data on the seasonality of lamb slaughter. **d**, Before mid-1988, both reported and unreported clinical BSE cases could be used for food (red-shaded curve). After that time, BSE was made notifiable and cases were destroyed, so we assume none entered food. The blue-shaded curve represents the rate of slaughter (per year) of pre-clinical infected cattle weighted by infectiousness relative to disease onset, assuming infectiousness grows at the exponential rate of 4 per year. The over-30-month scheme ended most bovine exposure in 1996, with estimates of residual levels (inset) being dependent on the extent of maternal transmission of BSE. The solid black curve represents the estimated infection hazard to cattle and sheep posed by infectivity in contaminated feed, relative to the maximum level reached in 1988.

Key to our analysis is estimates of the infectivity in animal tissues during disease incubation. Data are limited for BSE in sheep acquired by oral challenge, but using new experimental results and published data from studies of both scrapie⁴⁻⁷ and sheep BSE^{8,9} pathogenesis, we constructed an infectiousness profile. This profile was based on temporal changes in the density of the agent in different tissues, weighted by the proportion of such tissue in the host's body (Fig. 1b). This profile differs from that of BSE in cattle^{10,11}, with a more rapid rise in overall infectivity early in the incubation period in a wide range of tissues (for example, spleen and lymph nodes). The sheep-human infectiousness profiles (Fig. 1b) adjust for tissue-specific usage in food¹² and the effect of the 1997 specified risk materials (SRM) ban in sheep.

中 BSE 的患病率上限是 2%；图 1a)，并且要求与对这些绵羊群曾经与肉类和骨粉 (MBM) 接触的历史评估大致一样^[3]。

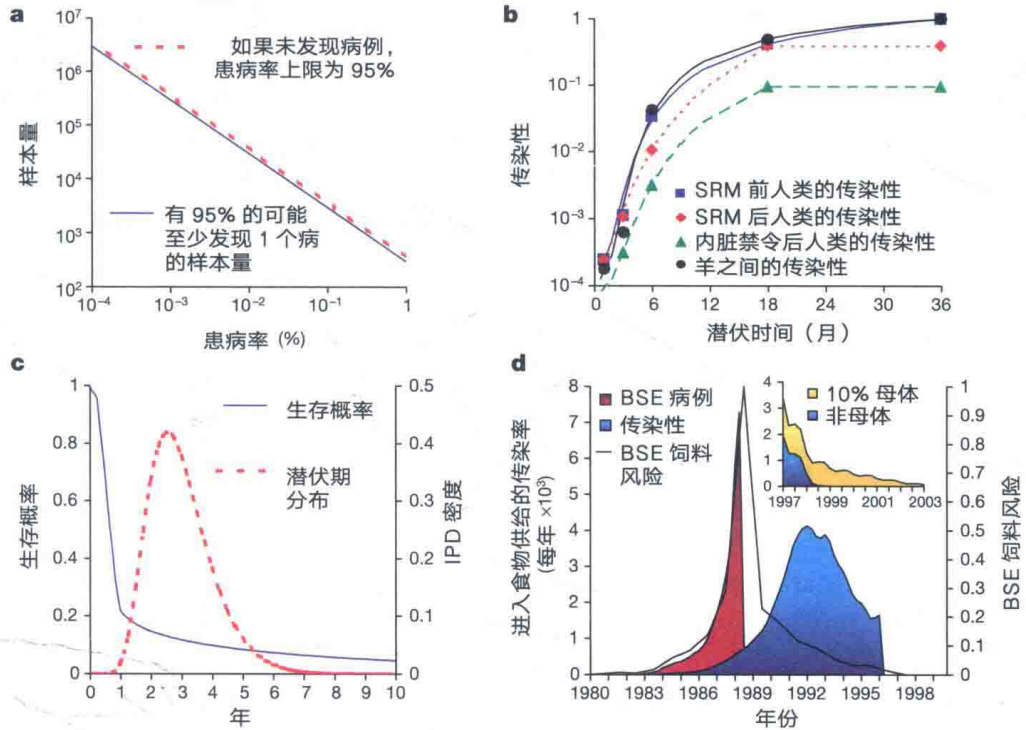


图 1. 传播模型中的流行病学数据。a, 在筛选研究中样本量和检测到的患病率间的关系。b, 羊传染性随感染时间的变化 (见方法)。羊和人的患病率概况分别归一化到最大值为 1。c, 羊随着年龄增长的生存概率, 以及假设的羊群中 BSE 的潜伏期分布状况 (IPD)。生存函数是根据每年 6 月份进行的羊群普查、屠宰、出口和失踪的数据以及羊羔屠宰的季节性数据进行估计的。d, 1988 年中期之前, 报告的和未报告的 BSE 患病牲畜都可以做成食品 (红色阴影曲线)。此后, BSE 病例都要上报, 并且牲畜都被销毁, 因此我们假定没有牲畜做成食品。蓝色阴影曲线表示临床感染前期牛的屠宰率 (每年), 以相对于疾病发病的传染性来表示, 假设传染性以每年 4 的速度指数式增长。这个超过 30 个月的方案在 1996 年结束了大部分牛群的暴露, 而残存水平的估计 (插入图) 取决于 BSE 母体传播的程度。黑色的实线表示相对于 1988 年达到的最高水平, 在受污染饲料中的传染性对牛羊造成的感染风险的估计。

我们分析的关键是评估疾病潜伏期内动物组织的传染性。通过进食感染的 BSE 羊群的数据有限, 但是根据对瘙痒病^[4-7]和羊 BSE^[8,9]发病机理研究所获得的新的研究结果和公布的数据, 我们构建出了一个传染性的概况。这个概况基于不同组织中病原体密度的暂时性改变, 以该组织在宿主体内所占的比例来表示 (图 1b)。此概况与牛中的 BSE 感染情况不同^[10,11], 表现为在不同组织 (例如脾和淋巴结) 的潜伏期早期, 总体传染性增加更快。羊-人传染的概况 (图 1b) 根据食物中特殊组织的含量^[12]以及 1997 年针对羊的高风险食品 (SRM) 禁令的效果进行调整。

The distribution of the BSE incubation period in sheep is not well characterized, but on the basis of the limited available data, we used an offset gamma distribution with a mean of 3 years (Fig. 1c) and substantial variance (intended to capture variation caused by dose dependency and host genotype) both for sheep infected by feed and those infected horizontally. Pathogenesis and susceptibility are dependent on the genetic background of the host¹³⁻¹⁵, and genotype frequencies of the key polymorphisms vary considerably within and between flocks of different breeds^{16,17}. Collation of limited available data suggests that roughly one-third of sheep in Great Britain (England, Scotland and Wales) have BSE-susceptible genotypes (see Supplementary Information). Exposure of the sheep flock to the BSE agent via contaminated feed (Fig. 1d) is assumed to mirror (albeit at a much lower level) that of British cattle, as estimated in back-calculation analyses of the BSE epidemic^{18,19}. Exposure is likely to have occurred as far back as the early 1980s, before the disease was identified in cattle^{18,19}. As for BSE in cattle²⁰, host survivorship is important given the long incubation period of the disease. Best estimates (see Supplementary Information) are presented in Fig. 1c (giving a mean life expectancy of 1.5 years), although more precise data are urgently required, perhaps based on a sheep equivalent of the British Cattle Tracing System (<http://www.bcms.gov.uk>).

Capturing the information in Fig. 1 requires a framework that integrates the temporal evolution of BSE pathogenesis in the individual host (incorporating age-dependent susceptibility and exposure) into a mathematical model of transmission within (including seeding and spread) and between flocks. This model builds on previous analyses of within- and between-flock transmission of scrapie^{21,22}, and consists of a set of nonlinear partial differential equations detailing the transmission dynamics of the agent and the demography of the sheep flock under time-dependent exposure to BSE-contaminated feed. The dynamics of disease transmission within the sheep population are determined by the magnitude of the respective basic reproduction numbers of the agent within a flock (R_0^A) and between flocks (R_0^F). The reproduction numbers define the average number of secondary cases or flocks generated by one primary case or infected flock in a susceptible flock or population of flocks. We considered three representative scenarios: (I) $R_0^A > 1$, $R_0^F < 1$ —self-sustaining transmission within a flock but not between flocks; (II) $R_0^A > 1$, $R_0^F > 1$ —the worst-case scenario for future spread, with spread within and between flocks inducing an expanding epidemic; and (III) $R_0^A < 1$, $R_0^F < 1$ —the best-case scenario, with non-self-sustaining transmission both within and between flocks (see Fig. 2 for precise parameter values).

For each scenario, the level of flock infection due to MBM exposure was adjusted to give BSE prevalence below 2% of scrapie prevalence at present (consistent with the results of ongoing studies screening sheep brains). Judgements of scenario consistency therefore depend on the estimated prevalence of scrapie in British sheep, with such estimates being based on limited data from detailed surveys of specific flocks (using clinical criteria for diagnosis) and a postal survey of farmers intended to characterize national historical patterns of scrapie incidence^{23,24}. The uncertainties in interpreting these data (giving estimates of infection prevalence anywhere between 0.1% and 1%, see Supplementary

羊群中 BSE 潜伏期的分布没有很明显的特征，但是根据有限的可用数据，我们对饲料感染以及水平感染的羊均使用平均数为 3 年的偏移 γ 分布 (图 1c) 以及显著的差异 (试图发现由剂量依赖性和宿主基因型引起的变化)。发病机制和易感性由宿主的遗传背景决定^[13-15]，重要多态性的基因型频率在不同品种的羊群内部和羊群之间的差别相当大^[16,17]。对有限可用数据的整理表明，英国 (英格兰、苏格兰和威尔士) 大约三分之一的羊具有 BSE 易感基因型 (见补充信息)。正如对 BSE 流行病的反算法分析所估计的那样，这些羊群通过污染的饲料暴露于 BSE 病原体中 (图 1d)，这与英国中的情况差不多 (尽管水平要低得多)^[18,19]。暴露很可能在 20 世纪 80 年代早期就已经存在，那时尚未在牛群中发现此病^[18,19]。对于牛的 BSE^[20]，由于潜伏期很长，宿主的生存概率就显得很重要。尽管迫切需要更加精确的数据，但图 1c 已经显示了最佳估计值 (见补充信息) (平均预期寿命是 1.5 年)，这可能基于在羊群中使用的英国牛群追踪系统 (<http://www.bcms.gov.uk>)。

获得图 1 所示的信息需要一个模型，而这个模型能够将个体宿主中 BSE 发病机制的时间演变 (包括年龄依赖的易感性和暴露) 整合到羊群内部 (包括播种和传播) 和羊群之间传播的数学模型中。该模型基于先前对羊群内部和羊群之间瘙痒病传播的分析^[21,22]，并且由一组非线性偏微分方程组成，详细描述了病原体传播的动力学和暴露在受 BSE 污染饲料下的具有时间依赖性的羊群的种群统计学。羊群中疾病传播的动力学是由群内部 (R_0^i) 和群之间 (R_0^e) 病原体各自的基础繁殖数量的大小决定的。繁殖数目定义了以下四种情况的平均数量，或者次要病例，或者由一个主要病例产生的羊群，或者易感群体中受感染的群体，或者种群。我们考虑了三个代表性情况：(I) $R_0^i > 1$, $R_0^e < 1$ ——群内部是自我维持的传播，而群之间不是；(II) $R_0^i > 1$, $R_0^e > 1$ ——未来最差的情况，在群内部和群之间传播，导致流行病不断扩大；(III) $R_0^i < 1$, $R_0^e < 1$ ——最好的情况，群内部和群之间都是非自我维持的传播 (精确的参数值见图 2)。

对于每一种情况，由于 MBM 暴露导致的群体感染的水平都调整到使得 BSE 的患病率低于目前 2% 的瘙痒病患病率 (与正在进行的羊脑筛查的研究结果一致)。因此，对情况一致性的判断就取决于英国羊群中估计的瘙痒病患病率，而这个估计是基于对特定羊群 (使用临床诊断标准进行诊断) 的详细调查以及对农民的邮政调查所得到的有限数据，目的是描述全国瘙痒病发病的历史模式^[23,24]。解释这些数据的不确定性 (感染的患病率估计值在 0.1% ~ 1% 之间，见补充信息) 使得大规模 (图 1a)

Information) make large-scale (Fig. 1a) screening of the national flock for transmissible spongiform encephalopathies (TSEs) a priority. In constructing the scenarios, we assumed a scrapie prevalence of about 0.3%, with scenarios II and III then corresponding to a BSE prevalence of 0.5% that of scrapie, and scenario I to a prevalence of about 2% that of scrapie. Scenario I was thus intended to represent something of a worst case in terms of the numbers of animals infected to date, although we cannot exclude the possibility of even larger epidemics given the limited data currently available.

Figure 2 displays the epidemiological characteristics of these scenarios in terms of within-flock and overall prevalence (Fig. 2a–c), and their implications for human exposure via food (Fig. 2d–f). The estimates of exposure incorporate data on human consumption of ovine material (see Supplementary Information), which indicate that 67% of lambs and 83% of sheep older than 12 months slaughtered for consumption in 1999 were consumed domestically in the UK. Very few live sheep are imported into Great Britain, and most imported lamb meat originates from New Zealand, which has never detected signs of BSE or scrapie infection in either its bovine or ovine populations. Thus the potential risk from BSE-infected sheep arises from home-bred animals.

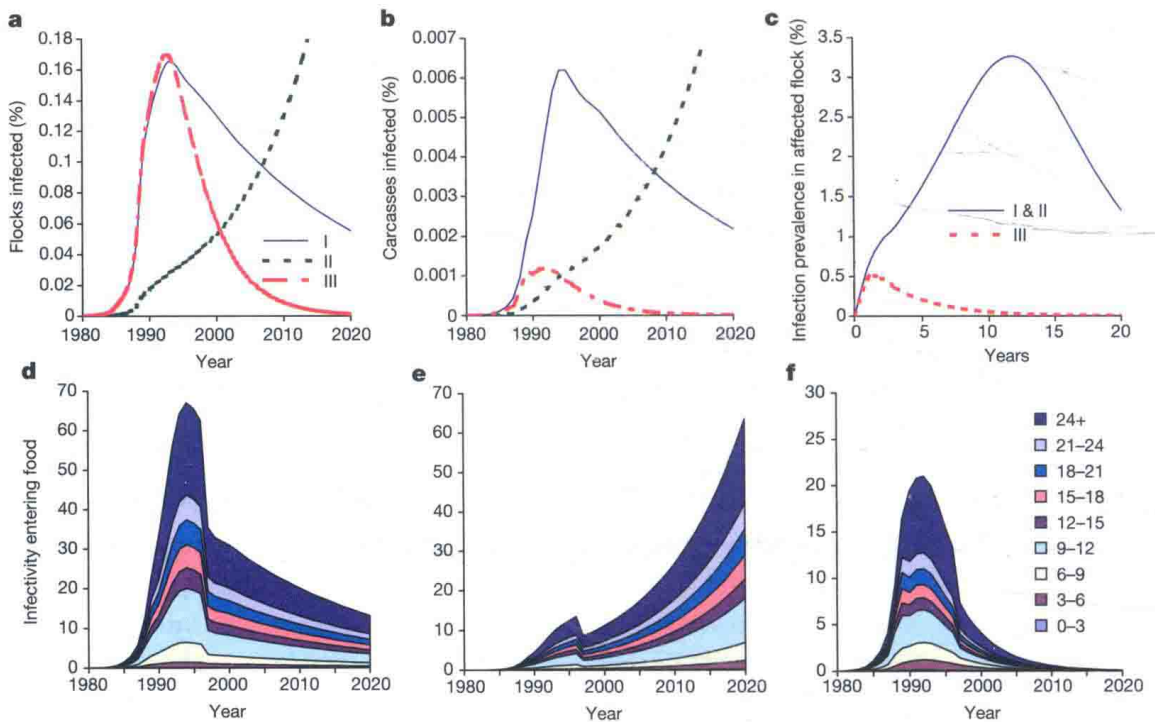


Fig. 2. Epidemiological characteristics of BSE transmission scenarios in sheep. $R_{\hat{\delta}} = 2$, $R_{\hat{\delta}}^{\text{I}} = 0.8$ and $\beta_{\text{B}} = 0.2\%$ per year for scenario I; $R_{\hat{\delta}} = 2$, $R_{\hat{\delta}}^{\text{II}} = 1.5$ and $\beta_{\text{B}} = 0.025\%$ per year for scenario II; $R_{\hat{\delta}} = 0.8$, $R_{\hat{\delta}}^{\text{III}} = 0.5$ and $\beta_{\text{B}} = 0.2\%$ per year for scenario III; where β_{B} is assumed flock infection incidence rate per unit of feed risk profile shown in Fig. 1c. By comparison, β_{B} values of 0.2% and 0.025% represent per-animal infection hazards about 50- and 400-fold less than that experienced by cattle. **a**, Proportion of flocks affected through time for scenarios I–III. **b**, Proportion of carcasses entering the food supply infected (at any incubation stage) with BSE. **c**, Prevalence in affected flock as a function of time since initial entry of infection into the flock. **d–f**, Estimated infectivity (in units of maximally infectious carcasses) entering the food supply under scenarios I, II and III, respectively, derived from the infectiousness profiles shown in

筛查全国羊群中的传染性海绵状脑病 (TSE) 成为优先事项。在构建上述情况时, 我们假定瘙痒病的患病率大约是 0.3%, 情况 II 和 III 相对应的 BSE 的患病率是瘙痒病的 0.5%, 而情况 I 对应的 BSE 患病率是瘙痒病的 2%。因此, 情况 I 预期能够代表目前为止感染动物数量的最差状况, 尽管我们不能排除由于目前可用的数据有限而发生更大范围流行病的可能性。

图 2 显示了这些情况在群内部和总体患病率方面的流行病学特征 (图 2a~2c), 以及它们在人类通过食物暴露时的影响 (图 2d~2f)。暴露估计包括人类对绵羊身体组成部分进行消费的数据 (见补充信息), 这表明 1999 年屠宰的 67% 的羊羔和 83% 的超过 12 个月龄的绵羊都是在英国国内消费的。很少有活羊进口到英国, 大部分进口的羔羊肉来自新西兰, 而新西兰从未在羊群或者牛群中检测到 BSE 或者瘙痒病感染的迹象。因此, BSE 感染的羊的潜在风险都来自于家养动物。

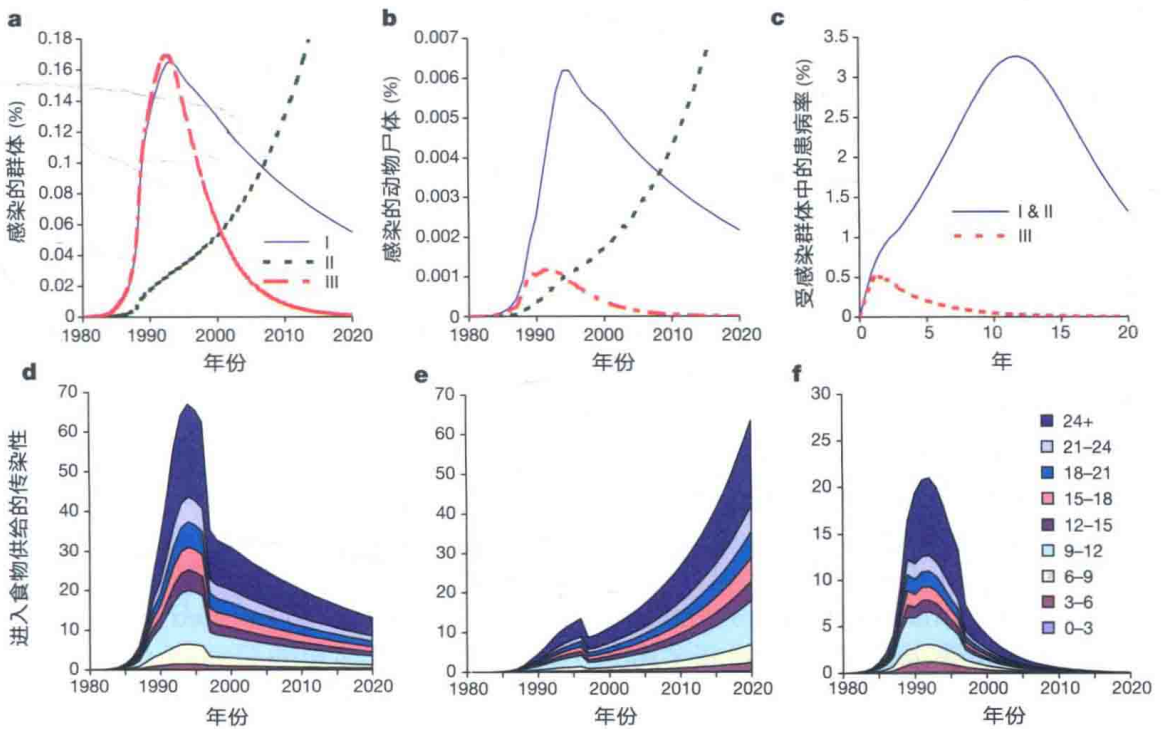


图 2. 羊群中 BSE 传播情况的流行病学特征。情况 I, $R_0^i = 2$, $R_0^e = 0.8$, $\beta_B = 0.2\%$ 每年; 情况 II, $R_0^i = 2$, $R_0^e = 1.5$, $\beta_B = 0.025\%$ 每年; 情况 III, $R_0^i = 0.8$, $R_0^e = 0.5$, $\beta_B = 0.2\%$ 每年; 其中 β_B 是每单位饲料风险分布的假定群体感染发病率, 如图 1c 所示。相比之下, β_B 值为 0.2% 和 0.025% 分别表示每个动物感染的风险是牛感染的风险的五分之一和四百分之一。a, 三种情况下, 随着时间的推移, 受感染群体的比例。b, 感染了 BSE 的动物尸体进入食物供给的比例 (包括各种潜伏阶段)。c, 从感染进入群体开始, 受感染群体的患病率随时间的变化的函数。d~f, 根据图 1a 所示的传染性概况, 在 I、II、III 三种情况下进入食物供给的估计传染性 (以最大传染性尸体为单位)。改变受 BSE 感染的羊群的不同比例